

Mechanical behavior of nano-copper interconnects subjected to thermal loading

M. Fidalgo

monica.fidalgo@tecnico.ulisboa.pt

Instituto Superior Técnico, Universidade de Lisboa, Portugal

May 2019

Abstract— As electronic components are continuously downscaled, Joule heating plays an increasingly critical role in the degradation or even failure of electric components. The high temperatures observed in such devices challenge the creation of smaller circuits and compromise their performance. In this context, it is crucial to understand the way thermal loading and silicon integrated circuit architectures influence stresses in nano-copper interconnect lines. The goal of this work is to produce a Finite Element (FE) model capable of predicting the thermal stresses at interconnect lines and use it to study the influence of different geometric parameters on the thermal stresses and deformation observed in copper lines. The FE analysis software Abaqus™ was used to simulate the integrated circuit's working conditions and an initial bidimensional approach was used for a reference configuration from which several geometric features were studied (line width, aspect ratio and line distance) and trends between the model architecture and stresses were established. Finally, a three-dimensional model was developed, and the results were compared with the bidimensional studies. In the present work, the bidimensional model was confirmed to provide matching results, as compared with 3D, for architectures with thicknesses above 40µm. Stresses at the copper lines were found to stabilize for aspect ratios higher than 1.5 and line distances higher than their respective width. Configurations with smaller line widths are subjected to higher compressive stresses. The results obtained from these models can provide useful guidelines for the optimal design of circuits.

Keywords— *copper interconnects, thermal loading, finite element method, residual stresses*

I. INTRODUCTION

As the demand for higher computational power has been increasing, electronic components have been continuously downscaled. In the context of these electronic components, interconnects (IC) are wires (stacked in multi-levels and with various line widths), responsible for transmitting signal, power and connecting various components within integrated circuits (IC). As of 1997, copper had become the metal of choice for IC. Due to the narrow line widths (currently at the nanometer scale), Joule heating plays an increasingly critical role in the degradation or even failure of components, such as microprocessors. The high temperatures observed in those devices are a challenge for creating smaller circuits without compromising their performance. When circuits are subjected to Joule heating under normal working conditions, the mismatch between the thermal expansion coefficient of copper and all other materials present in the IC promotes the development of thermal stresses, which pose a serious threat to IC performance. In this context, it is paramount to understand the way thermal loading and silicon integrated circuit architectures influence stresses in nano-copper interconnect lines.

Many approaches can be taken to address this problem, such as testing, characterization or modelling. In this study, a modelling approach by means of the Finite Element (FE) method is featured and Abaqus™ was the Finite Element Analysis (FEA) software chosen.

The finite element method has been a tool for modelling stresses in metal interconnects before the introduction of copper in the semiconductor industry. Studies about the effects of line distance and aspect ratio in periodic aluminum interconnect lines of very simple geometry were performed by Y. -L. Shen in 1997. Shen realized that the effects of line aspect ratio on stresses are not independent of the spacing between lines [1].

A more recent study regarding copper interconnects concluded that the stiff barrier layers surrounding the copper lines promote stress accumulation at the corners, which is likely to stimulate electromigration and voiding [2]. This study was performed for annealing conditions and used experimental data from copper thin films to model plastic strain hardening in encapsulated copper films. The experimental results suggested that treating copper as an elastic-perfectly plastic solid with temperature-dependent yield strength (as was usually the practice for Aluminum) could come at the cost of significant errors in stresses generated inside the copper lines.

The intersection of the barrier layer and the copper line was again confirmed to play a vital role in void formation, when a study by Wei Li et al. analyzed the dynamic physical processes of EM such as void nucleation and void growth [3]. Vacancies moving through the grain boundaries become immobilized at that intersection due to its higher strain energy (higher stresses at this intersection are a consequence of the thermal mismatch of the different materials present). Since the movement and nucleation of vacancies occurs to reduce the strain energy, the barrier layer-grain boundary intersections are the weakest points for the void formation in metal interconnects.

A study of the effects of grain structures on the rate of electromigration-induced failure of copper interconnects was performed, by C. S. Hau-Riege and C. V. Thompson, using scanned laser annealing (SLA) to produce interconnects with different grain structures. Electromigration experiments carried out on copper interconnects with very different grain structures showed no significant differences in failure rates, which suggested that electromigration in copper interconnects with standard liners and interlevel diffusion-barrier layers occurs by mechanisms which are faster than grain boundary self-diffusion [4]. C.-K. Hu et al. compared the effects of electromigration in copper interconnects with different capping layers. According to the study's conclusions, a thin Ta/TaN cap on top of the copper line surface improves electromigration lifetime more effectively than a SiNx or SiCxNyHz cap. The activation energy for electromigration was shown to have

increased from 0.87eV for cap-less lines to 1.0-1.1eV for SiNx or SiCxNyHz caps and 1.4eV for 1.4 eV for Ta/TaN capped samples [5].

Depending on the orientation, dimensions, surroundings, and location of the grains, thermally stressed copper lines can be subjected to very significant variations ($\times 10$) in normal stresses along the grain boundaries [6]. Normal stresses observed in copper interconnect lines can thus become higher depending on the orientation of the grains, introducing weak points inside the metal lines where delamination and accumulation of vacancies is most likely to occur. Annealing and polishing treatments can significantly alter the texture and strain observed in copper damascene lines [7].

An expeditious method to analyze local texture, local stress and stress gradients in copper interconnect lines with small width-to-thickness ratios is exemplified by K. J. Ganesh et al [8]. An automated scanning transmission electron microscope (STEM) diffraction technique was used to map the local grain orientation of 120nm wide copper interconnect lines, after which an Objected Oriented Finite Element Method software for microstructure analysis (OOF2) is used to analyze the local stresses.

In the present study, the main goal was to produce a finite element model capable of predicting the thermal stresses occurring in copper interconnect lines and subsequently use it to study the influence of geometric parameters, such as line width, aspect ratio and distance between lines on thermal stresses and deformation observed in copper lines. This work's original contributions are centered around the simulation of the IC's critical working conditions (instead of annealing conditions) and a detailed examination and discussion of different geometries, material modelling options and their implications. Thermal stresses are examined both at maximum (critical) temperature and at room temperature after cooling (residual stresses).

An initial bidimensional approach with plane strain configuration was used for a base-model with a line width 180nm and aspect ratio 1.5. This base model's architecture was based on a test structure from Freescale Semiconductor, Inc. TM found on a 2007 paper from Mei et al. [9]. Based on this reference configuration, several geometric features were studied, such as different combinations of line widths, aspect ratios and line distances, so that trends between the architecture of the lines and stresses could be established. Different constitutive models concerning material behavior were tested against each other (pure elasticity, ideal plasticity, work-hardening). The multidimensionality of the problem and its consequences are also discussed in detail. Finally, a three-dimensional model was developed, and the results were compared with the bidimensional studies to validate the latter, justifying its application.

II. METHODOLOGY

There is a wide range of different architectural choices for interconnect lines, and different levels of interconnectors can have increasingly more complex three-dimensional geometries. In the interest of this study, a specific architecture was chosen as base-model from which slightly different variations are performed.

The architecture chosen is mostly based on the multilayer copper interconnect structure from a 2007 paper by Mei et al

[9] but the aspect ratio (length/width) was set to 1.5 for greater simplicity. The cross-section of the problem is represented in Fig.1. The base configuration line width is 180nm and is equal to the distance between interconnect lines. The capping and passivation layers are 0.25 μm and 0.05 μm long, respectively, and the diffusion barrier is 0.01 μm thick.

The periodicity of the cross-section allows it to be modelled as mirrored and patterned repetition of a unit cell (Fig.1) if a proper symmetry condition is set along its side walls (no displacement allowed in the 1-direction). The list of materials used in the model is also shown in Fig.2.

A total of six constitutive models are used throughout this work. For pure elastic regime models:

(i) Elast1: All materials are linear elastic solids whose properties are shown in Tab.1 [9] [10].

(ii) Elast2: Same as "Elast1", but copper's coefficient of thermal expansion (CTE) is treated as temperature-dependent in accordance with Tab.2 [11].

For plastic regime models:

(iii) IdPlast: Same as "Elast2", but copper's yield stress is treated as temperature-dependent in accordance with Tab.3 [11]. In other words, copper is treated as an isotropic elastic-perfectly plastic solid while the rest of the model undergoes no plastic deformation.

(iv) WHardCu: Same as "Elast2", but copper undergoes non-temperature dependent work-hardening while the rest of the model undergoes no plastic deformation. The true stress-strain curve used for copper (at 20°C) is shown in Fig.3 [11].

(v) WHard: Same as "Elast2", but the entire model undergoes non-temperature dependent work-hardening and the true stress-strain curves used for each material (at 20°C) are shown in Fig.3-7 [9] [10] [11] [12].

(vi) Plast: Same as "Elast2", but copper and tantalum undergo temperature dependent work hardening and the true stress-strain curves of these two materials are shown in Fig.3 [9] [11] and FIG.4 [10] [12]. The rest of the model undergoes non-temperature dependent work-hardening and the true stress-strain curves used (at 20°C) are shown in Fig.5-7 [9] [10].

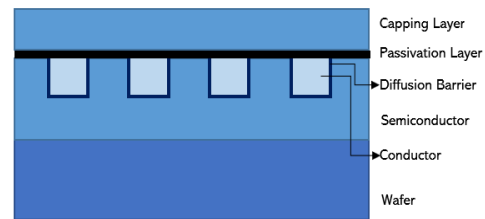


Fig.1 Cross-section of the problem

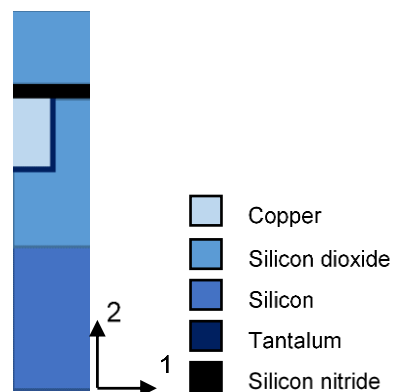


Fig.2 Unit cell and materials present in the model

TABLE I. MATERIAL PROPERTIES USED FOR COPPER IN "ELAST1" AND FOR ALL OTHER MATERIALS IN THE REST OF THE MODELS

| Material | CTE ($\times 10^{-6}$) | Young's Modulus (MPa) | Poisson Ratio |
|----------------------|--------------------------|-----------------------|---------------|
| Silicon [9] | 4.2 | 165 000 | 0.22 |
| Silicon Dioxide [10] | 0.55 | 68 000 | 0.15 |
| Silicon Nitride [9] | 2.9 | 290 000 | 0.27 |
| Tantalum [10] | 6.6 | 183 000 | 0.35 |
| Copper [9] | 17 | 128 000 | 0.36 |

TABLE II. COEFFICIENT OF THERMAL EXPANSION USED FOR COPPER IN ALL MODELS EXCEPT "ELAST1"

| Material | Temperature (°C) | CTE ($\times 10^{-5}$) |
|-------------|------------------|--------------------------|
| Copper [11] | 20 | 1.54 |
| | 27 | 1.54 |
| | 77 | 1.58 |
| | 100 | 1.59 |
| | 127 | 1.62 |
| | 177 | 1.65 |
| | 200 | 1.66 |
| | 227 | 1.69 |
| | 277 | 1.73 |

TABLE III. YIELD STRESS VALUES USED FOR COPPER IN MODEL "IDPLAST2"

| Material | Temperature (°C) | Yield Stress (MPa) |
|-------------|------------------|--------------------|
| Copper [11] | 20 | 211 |
| | 100 | 205 |
| | 200 | 195 |
| | 250 | 170 |

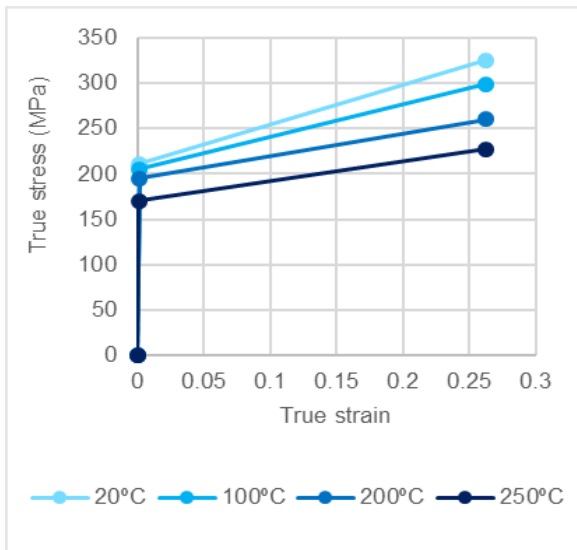


Fig.3 True stress-strain curves of Copper at different temperatures

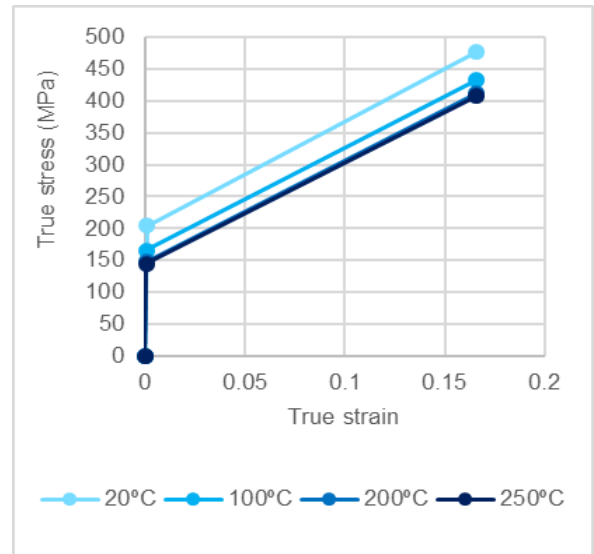


Fig.4 True stress-strain curves of Tantalum at different temperatures

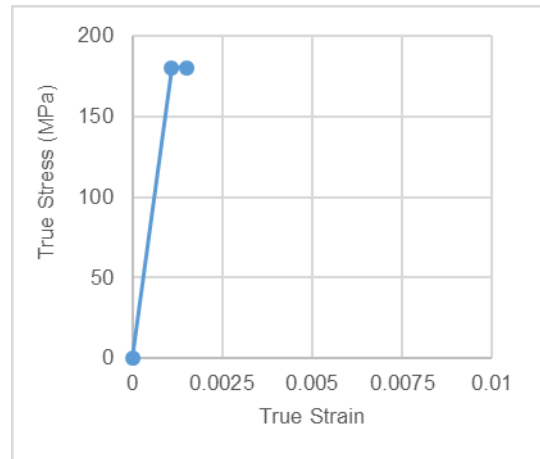


Fig.5 True stress-strain curve of Silicon at 20°C

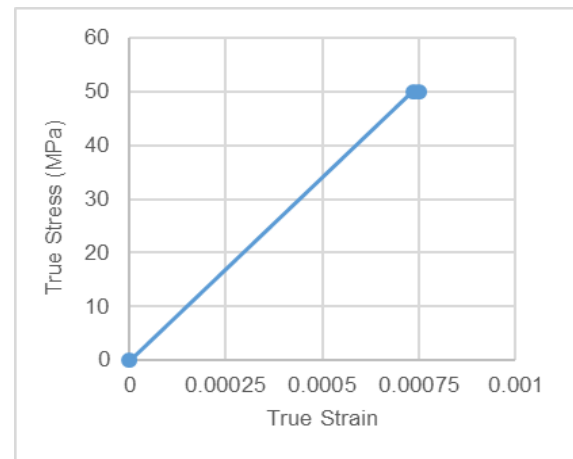


Fig.6 True stress-strain curve of Silicon dioxide at 20°C

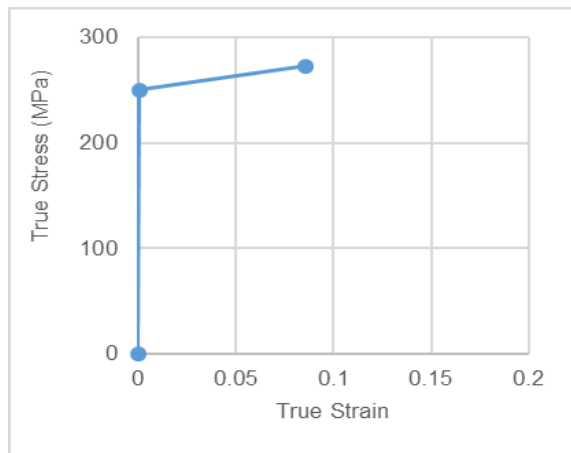


Fig.7 True stress-strain curve of Silicon nitride at 20°C

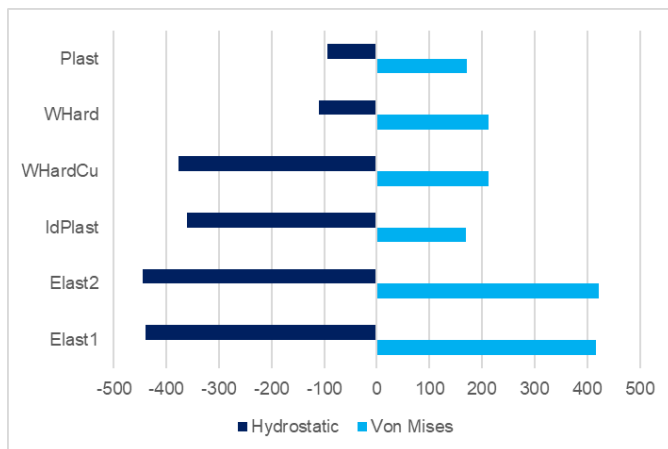


Fig.8 Von Mises and hydrostatic stress values (MPa) at control point B for all constitutive models, at t=1s

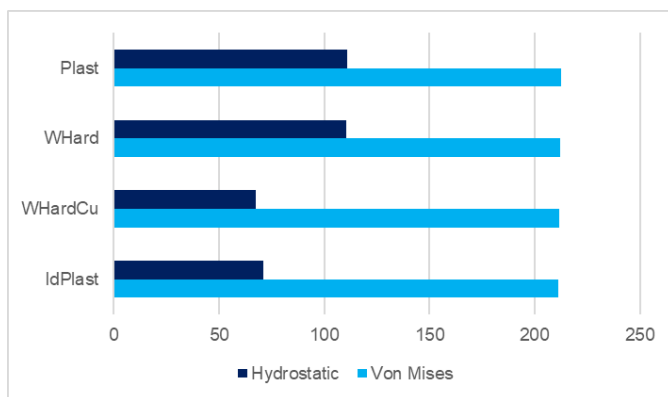


Fig. 9 Von Mises and hydrostatic stress values (MPa) at control point B for all plastic constitutive models, at t=2s

The thermal load is simulated through a global (isothermal) application of a 1 second heating step ($\Delta T = 230^{\circ}\text{C}$) from room temperature, 20°C , to a maximum temperature of 250°C ; followed by a 1 second cooling back to room temperature.

A symmetry boundary condition is used to simulate the periodicity of the copper lines. The top surface is free to move during deformation and the bottom surface is pinned to prevent rigid body motion. These loading and boundary conditions are unchanged for every study elaborated in the scope of this work and results will always be observed at either $t=1\text{s}$ (maximum temperature) or $t=2\text{s}$ (after cooling).

The initial stress distribution present in the model is zero and all materials are treated as isotropic. For all bidimensional studies, plane strain finite elements are used.

After a thorough convergence study, an appropriate mesh with linear quadrangular plane strain elements of global size $0.005\mu\text{m}$ was chosen for the bidimensional models. For the three-dimensional models, a linear hex biased mesh of $0.02\mu\text{m}$ size around the copper lines and $0.05\mu\text{m}$ in the rest of the model was used.

III. RESULTS AND DISCUSSION

A study to test all six constitutive models was elaborated. The values of the Von Mises stress and hydrostatic stresses were taken at a representative point located on the geometric center of the unit cell's copper line (control point B) for each of the six constitutive models.

In the case of plastic constitutive models, results were taken at maximum temperature ($t=1\text{s}$) and after cooling ($t=2\text{s}$). For pure elastic regime results are taken only at $t=1\text{s}$, as no residual stresses occur in elastic simulations. The outcome of this study is shown in Fig.8 and Fig.9.

The results for models Elast1 and Elast2 are very similar for both Von Mises and hydrostatic stresses, so considering the CTE of copper constant or temperature dependent does not produce large differences in results. In models where only copper is considered plastic (IdPlast and WHardCu), the hydrostatic stress values observed at $t=1\text{s}$ (Fig.8) are lower than in the case of pure elasticity and higher than in globally plastic models (WHard and Plast). The residual hydrostatic stresses (Fig.9), however, are higher for the models where all materials can deform plastically.

For plastic constitutive models, the Von Mises stress values at $t=1\text{s}$ are similar for temperature independent plastic models (WHard and WHardCu) and higher than for temperature dependent plastic models (IdPlast, Plast), which are also approximately equal. The residual Von Mises stresses seem independent of the plastic model considered, so hydrostatic stresses will be the ones shown in upcoming geometry studies instead. Results are gravely influenced by different assumptions and, when modelling material behavior, constitutive models and other assumptions must be given great thought beforehand.

From the base model architecture presented in Fig.1-2, the width (1-dimension) of the interconnect lines was kept at 180nm, while the length (2-dimension) was changed to create different aspect ratios, $AR \in \{0.25, 0.4, 0.5, 0.6, 0.75, 1.0, 1.5$ (base model), $2.0, 2.5\}$, where $AR = \text{depth}/\text{width}$, while the other dimensions remained unchanged. The hydrostatic stresses present at control point B for different aspect ratios are plotted and compared in Fig.10 (maximum temperature) and Fig.11 (at the end of cooling), for all constitutive models.

There is a clear tendency for stresses to stabilize for aspect ratios greater than 1.5 (original model) independently of the constitutive model used. For constitutive models Elast1, Elast2, WHard and Plast; smaller aspect ratios translate to higher (compressive) hydrostatic stresses at $t=1s$ (Fig.10). For models IdPlast and WHardCu, however, smaller aspect ratios tend to decrease hydrostatic stresses. This distinct behavior comes from the fact that, in models IdPlast and WHardCu, only copper is considered plastic while all other materials were assumed perfectly elastic. The residual stresses (Fig.11) show approximately the same tendency for stabilization after aspect ratios higher than 1.5. Stresses behave likewise for all plastic models: at smaller aspect ratios, higher (positive) hydrostatic stresses are observed.

To study the influence of the distance between interconnect lines, all dimensions of the base-model except for the line distance are unchanged. The smallest distance between lines studied corresponds to the limit situation at which the distance separating the copper lines is equal to the thickness of the diffusion barrier and the upper limit studied corresponds to a distance six times greater than that of the base model. The original model has a line distance of $0.18\mu\text{m}$, equal to its line width.

The distances studied were $d = \{0.01, 0.03, 0.06, 0.09, 0.18$ (base model), $0.36, 0.54, 0.72, 0.9, 1.08\}$ (units in μm). The hydrostatic stresses present at the copper lines for different line distances tested are plotted and compared in Fig.12 (maximum temperature) and Fig.13 (at the end of cooling) for all constitutive models. Although the effects of line aspect ratio on stresses are not independent of the spacing between lines (Shen, 1997) [1], that does not invalidate this study's results. It should be noted, however, that this analysis corresponds to the specific case for which the spacing between lines is equal to the linewidth.

There is a tendency for stresses to stabilize for line distances greater than $0.18\mu\text{m}$ (which is the line distance and line width of the original model) for models Elast1 and 2, IdPlast and WHardCu. The stress curves for models WHard and Plast show a maximum (minimum absolute value) for a line distance of $0.09\mu\text{m}$ and stabilize for line distances greater than $0.54\mu\text{m}$. For model Elast1 and 2, smaller line distances increase (compressive) hydrostatic stresses at $t=1s$ (Fig.11). For models IdPlast and WHardCu, however, smaller line distances decrease hydrostatic stresses at $t=1s$. The residual stresses (Fig. 12) show the same tendency for stabilization for line distances of $0.54\mu\text{m}$ and beyond. Stresses behave likewise for models IdPlast and WHardCu, and a minimum stress is reached for a line distance of $0.18\mu\text{m}$ (original model). In models WHard and Plast, a similar tendency can be observed, but with overall higher residual stresses (when compared to models IdPlast and WHardCu) and hydrostatic stresses minimize at a line distance of $0.09\mu\text{m}$.

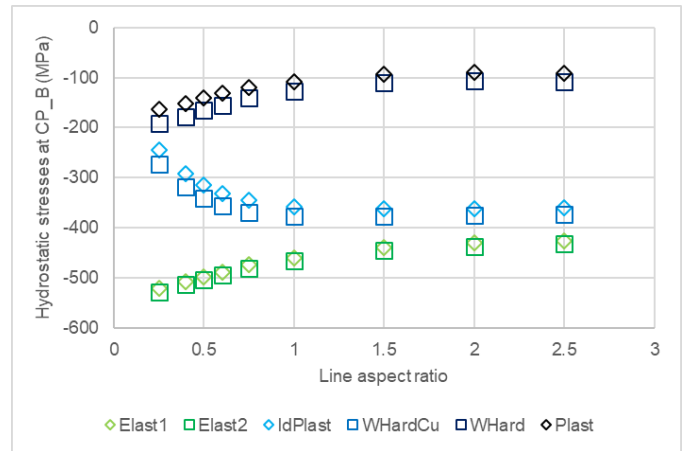


Fig.10 Results of the aspect ratio study for all constitutive models, at $t=1s$

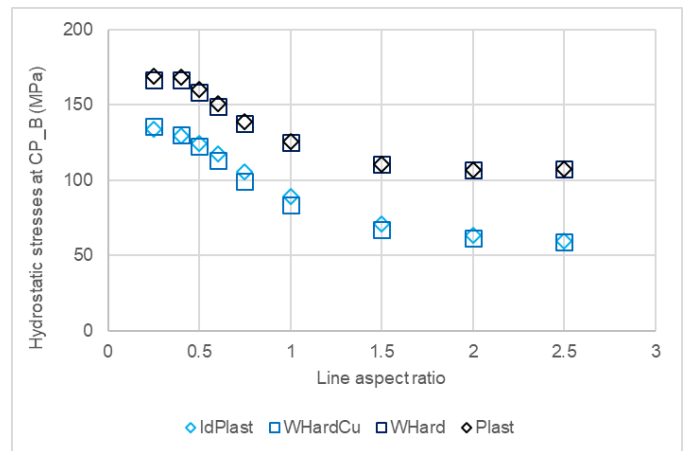


Fig.11 Results of the aspect ratio study for all plastic constitutive models, at $t=2s$

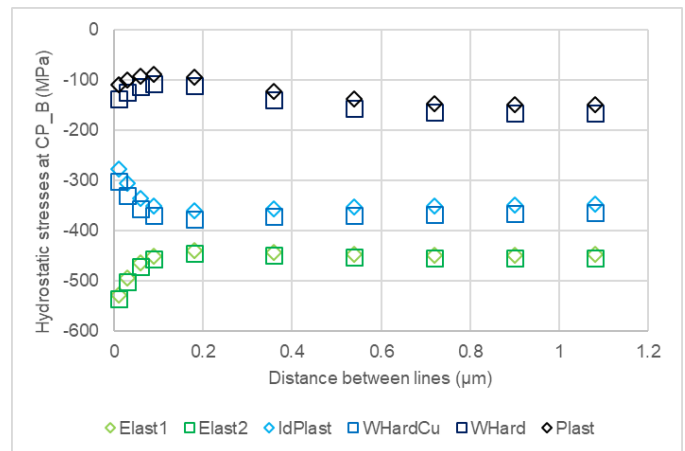


Fig. 12 Results of the line distance study for all constitutive models, at $t=1s$

Finally, the influence of line width in the stresses observed at the interconnect lines was studied. In order to keep the changes made between models used for this study as minimal as possible, the base-model (180nm line width) was slightly tweaked from an aspect ratio of 1.5 to 2.0 and the thickness of its tantalum diffusion barrier decreased from 10nm to 1nm. This way, the same aspect ratio and diffusion barrier thickness can be kept constant throughout all models with different line widths.

The distance between lines should not be kept constant throughout all models because not only does it influence the stresses observed at the interconnect lines, keeping a constant distance of 180nm would completely mischaracterize smaller geometries. The best compromise would be to keep the distance between lines always equal to the respective line's width. It is imperative for this study to keep the highest degree of familiarity possible between models so that a meaningful comparison between them can be made. For smaller linewidth models, keeping the base-model's length is unsustainable from a computational point of view if the same relative mesh size is to be kept. This problem was solved by dimensioning each model's length in direct proportion to the base-model's.

The hydrostatic stresses present at the copper lines for models with different line widths are plotted and compared in Fig.14 (maximum temperature) and Fig.15 (at the end of cooling) for all constitutive models.

There is a tendency for smaller line widths to increase (compressive) hydrostatic stresses independently of the constitutive model used, for $t=1s$ (Fig.14), i.e., models with smaller copper line width are subjected to higher compressive stresses when compared to architectures with larger widths.

The residual stresses are seemingly independent of line width for models IdPlast and WHardCu (Fig.15). For models WHard and Plast, the hydrostatic stresses are highest for smaller line widths. This distinct behaviour between plastic models is, again, a direct consequence of assuming, in models IdPlast and WHardCu, that only copper behaves plastically while the rest of the materials are in pure elastic regime.

In the bidimensional studies a plane strain working hypothesis was used. This simplification is frequently used for very thick models. The true model thickness (in the 3-direction) is an unknown but it would be reasonable to assume that the model would be at least as thick as it is lengthy (2-direction).

A representative line, CP_{edge} , was defined as the straight line perpendicular to the cross section of the three-dimensional model (parallel to the 3-axis) and whose origin is at representative point B. That is, the geometric centerline of the unit cell's interconnect line.

If the 2D model is to be verified by the 3D model, then as the size of the third dimension of the model is increased, the maximum stresses observed along CP_{edge} are expected to tend towards values like the ones obtained for the bidimensional analysis at representative point B (the geometric center of the unit cell's copper line).

Models with the same base geometry (cross-section shown in figures 1 and 2) and different thicknesses $Z \in \{1,4,8,12,16,20,32,40,50\}$ were created. The values of the Von Mises, S_{11} , S_{22} and S_{33} stresses, taken at the mid cross section, $Z=z/2$ (where stresses are higher) are represented in Fig.16-17 (for constitutive models Elast2 and Plast, respectively) next to their bidimensional (plane strain) counterparts. All stress values were taken at $t=1s$ (when the temperature is highest).

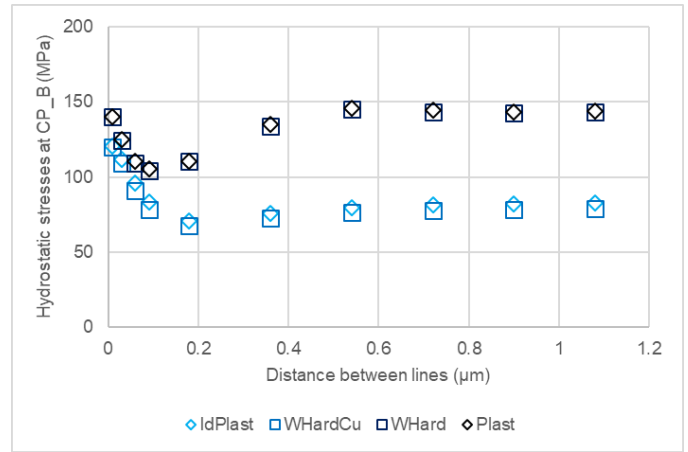


Fig. 13 Results of the line distance study for all plastic constitutive models, at $t=2s$

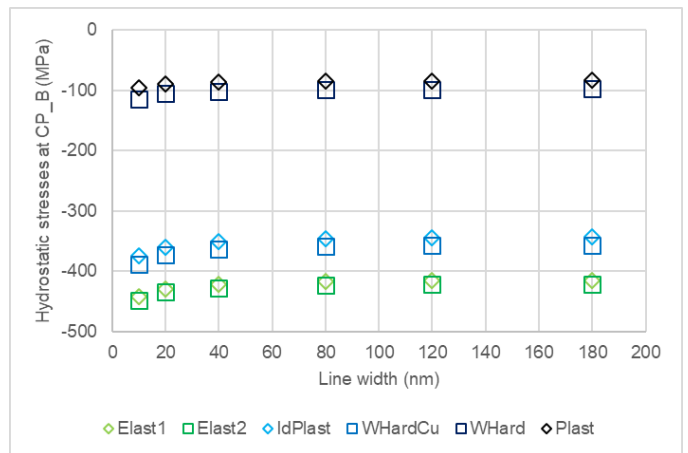


Fig.14 Results of the line width study for all constitutive models, at $t=1s$

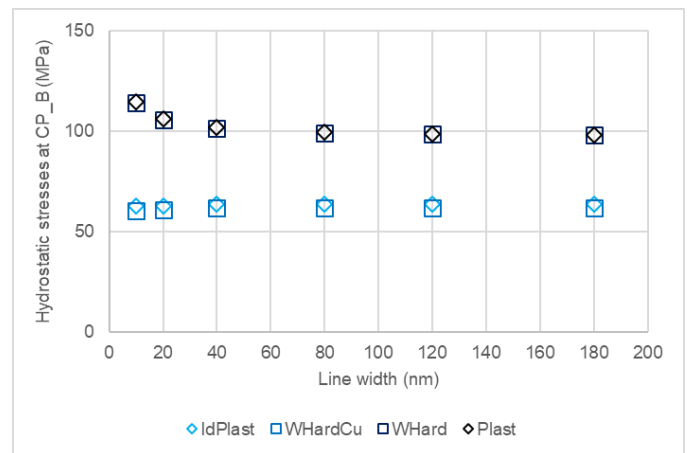


Fig. 15 Results of the line width study for all plastic constitutive models, at $t=2s$

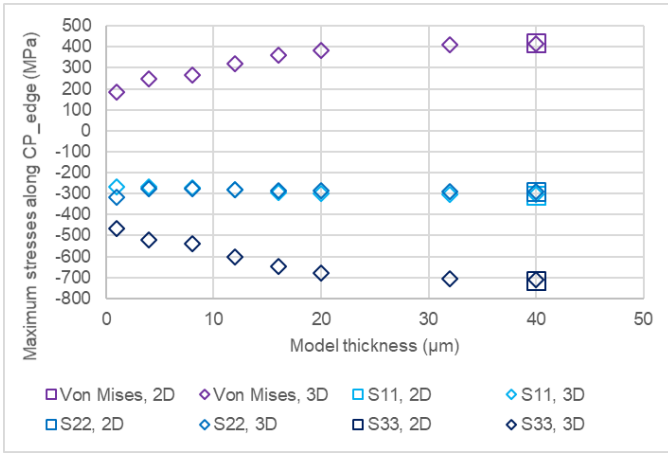


Fig.16 Comparison between the three-dimensional and bidimensional results, at t=1s, for constitutive model Elast1

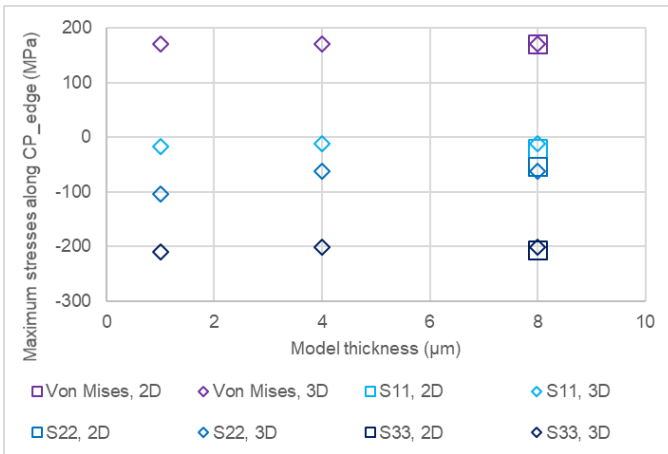


Fig.17 Comparison between the three-dimensional and bidimensional results, at t=1s, for constitutive model Plast

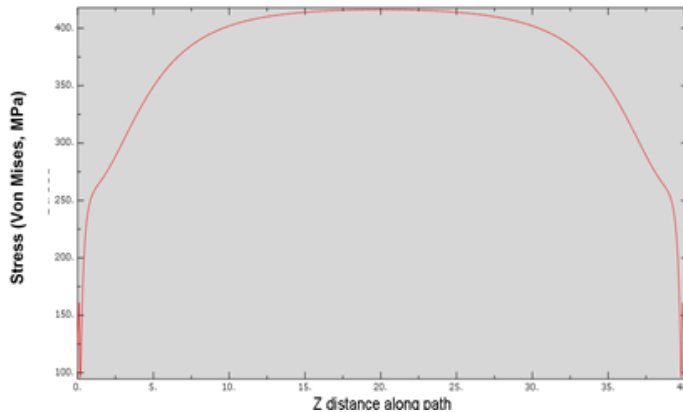


Fig.18 Stress (MPa) distributions at CP_{edge} along thickness z (μm) for a 3D model of total thickness 40μm (at t=1s, for constitutive model Elast1)

In Fig.16, the reliability of the elastic bidimensional model becomes clear for models of thickness equal or higher than 40μm. The same study performed for plastic conditions (model Plast) is shown in Fig.17, in which the 3D model tends to the bidimensional results faster, at Z=8μm. Overall these results confirm the reliability of the studies performed for the bidimensional models for 3D models of at least 40μm thickness.

The Von Mises stress distribution along CP_{edge} (at t=1s) are shown in Fig.18 for a three-dimensional model of thickness Z=40μm (Elast1 assumption was used). As previously mentioned, stresses observed at the free (front/back) surfaces (Z=0μm and Z=40μm, respectively) are the lowest and the model displays a symmetric stress distribution with the highest stress values registered at Z=z/2.

IV. CONCLUSIONS

The stress distributions observed in the interconnect lines are severely influenced by the constitutive model chosen. For very small thermal loads an elastic model can be considered, but in general a plastic model with temperature dependent strain hardening should be considered.

Von Mises stresses were much higher at the copper lines (≈ 420MPa) in the pure elastic regime (constitutive models Elast 1 and 2). For plastic models, Von Mises stresses at the copper lines were lower (≈ 170MPa) when the temperature dependency is considered (IdPlast and Plast) and higher (≈ 210MPa) when the model undergoes temperature independent work-hardening (model WHardCu and WHard).

On the assumption that the initial (t=0s) state of stresses is null, the entirety of the interconnect lines are subjected to negative (compressive) stresses when the temperature is at its highest. This is because copper possesses a significantly bigger CTE than all other materials present in the component, and thus when the copper lines try to expand due to the increase in temperature, their dilation is partially restricted by the surrounding materials, resulting in compression forces.

Several geometric features were studied to establish trends between the architecture of the lines and the stress distribution. In the line aspect ratio and distance studies, regardless of their initial behavior and independently of the constitutive model used, stresses were found to stabilize for aspect ratios and line distances greater than 1.5 and 0.18μm (0.54μm for models WHard and Plast), respectively. These results suggest that commercial circuits use aspect ratios and line distances that stabilize (and lower) thermal stresses in the interconnect lines. Models with smaller line widths are subjected to higher compressive stresses, at working temperatures, when compared to architectures with larger widths.

A three-dimensional model was created to test the bidimensional plane strain hypothesis. The highest stress values observed along CP_{edge} for a 3D model of enough thickness (which depends on the constitutive model considered) very closely match the ones observed at the geometric center of the unit cell's copper line in the bidimensional model. For plastic regime (Plast), the 3D stress values tend to the bidimensional stress values faster than for elastic regime (Elast1). The behaviors observed in bidimensional studies have a direct correlation to the ones potentially observed in their three-dimensional counterparts if

the thickness of the third dimension is equal to or higher than 40µm. This is advantageous in circuit design studies because CPU time for a 2D model is typically less than 5% as compared with 3D. Subsequently, the results obtained from these studies can provide useful guidelines for the optimal design of circuits.

ACKNOWLEDGMENT

The author acknowledges the help of Prof. Augusto Moita de Deus and Prof. Paulo J. Ferreira, as well as CeFEMA - Center of Physics and Engineering of Advanced Materials and INL – International Iberian Nanotechnology Laboratory.

REFERENCES

- [1] Y. -L. Shen, "Modeling of thermal stresses in metal interconnects: Effects of line aspect ratio," *Journal of Applied Physics*, vol. 82, no. 4, pp. 1578-1581, 1997.
- [2] E. EGE and Y.-L. SHEN, "Thermomechanical Response and Stress Analysis of Copper," *Journal of Electronic Materials*, vol. 32, no. 10, pp. 1000-1011, 2003.
- [3] W. Li, C. M. Tan and Y. Hou, "Dynamic simulation of electromigration in polycrystalline interconnect thin film using combined Monte Carlo algorithm and finite element modeling," *Journal of Applied Physics*, vol. 101, no. 104314, pp. 1-6, 2007.
- [4] C. S. Hau-Riege and C. Thompson, "Electromigration in Cu interconnects with very different grain structures," *Applied Physics Letters*, vol. 78, no. 22, pp. 3451-3453, 2001.
- [5] C.-K. Hu, L. Gignac, E. Liniger, B. Herbst, D. L. Rath, S. T. Chen, S. Kaldor, A. Simon and W.-T. Tseng, "Comparison of Cu electromigration lifetime in Cu interconnects coated with various caps," *Applied Physics Letters*, vol. 83, no. 5, pp. 869-871, 2003.
- [6] A. Basavalingappa and J. R. Lloyd, "Effect of Microstructure and Anisotropy of Copper on Reliability in Nanoscale Interconnects," *IEEE Transactions on Device and Materials Reliability*, vol. 17, no. 1, pp. 69 - 79, 2017.
- [7] B. Kaouache, S. Labat, O. Thomas and S. Maitrejean, "Texture and strain in narrow copper damascene interconnect lines: An X-ray diffraction analysis," *Microelectronic Engineering*, vol. 85, no. 10, pp. 2175-2178, 2008.
- [8] K. Ganesh, S. Rajasekhara, J. Zhou and P. Ferreira , "Texture and stress analysis of 120 nm copper interconnects," *Scripta Materialia*, vol. 62, no. 11, p. 843–846, 2010.
- [9] H. Mei, J. An, R. Huang and P. Ferreira, "Finite element modelling of stress variation in multilayer thin-film specimens for in situ transmission electron microscopy experiments", *Journal of Materials Research and Technology*, vol. 22, no. 10, pp. 2737-2741, 2007.
- [10] CES EduPack database, 2016.
- [11] Advanced Energy Technology Group - UC San Diego, "Pure Copper," [Online]. Available: <http://www-ferp.ucsd.edu/LIB/PROPS/PANOS/cu.html>. [Accessed November 2018].
- [12] S. R. Chen and G. T. Gray III, "Constitutive behavior of tantalum and tantalum-tungsten alloys," *Metallurgical and materials transactions A*, vol. 27A, pp. 2994-3006, 1996.